

Composite (multi)ferroic order

R. Matthias Geilhufe^{1,*}

¹*Department of Physics, Chalmers University of Technology, 412 96 Göteborg, Sweden*

(Dated: June 28, 2024)

The formalism of composite and intertwined orders has been remarkably successful in discussing the complex phase diagrams of strongly correlated materials and high- T_c superconductors. Here, we propose that composite orders are also realized in ferroelectric and ferromagnetic materials when lattice anisotropy is taken into account. This composite order emerges above the ferroic phase transition, and its existence is determined by the easy axis of magnetization or polarization, respectively. In multiferroic materials, where polarization and magnetization are coupled, composites of both orders are possible. This formalism of composite orders naturally accounts for magnetoelectric monopole, toroidal, and quadrupole orders. More broadly, composite orders may explain precursor phenomena in incipient (multi)ferroic materials, arising at temperatures above the ferroic phase transition and potentially contributing to the characterization of currently hidden orders.

INTRODUCTION

Condensed matter consists of a multitude of ions and electrons, often arranging themselves in regular patterns at low temperatures. Some ordering phenomena, such as crystalline, magnetic, or (anti)ferroelectric orders, have long been known and can be experimentally verified with high precision. Others, such as ferrotoroidicity[1–4], have remained more elusive. Composite orders are characterized by an order parameter $\langle AB \rangle$, composed of two observables A and B . Interestingly, composite orders can be non-zero $\langle AB \rangle \neq 0$ even if each individual order is not present, i.e., $\langle A \rangle = \langle B \rangle = 0$ [5]. Examples include odd-frequency pairing[6–8], composite $U(1)$ orders, such as those composed of 2-component superconducting order parameters[9–11], or 2-component bosonic systems[12, 13], and charge $4e$ superconductors[14, 15]. Recent experiments support the existence of composite orders[16, 17]. A point group symmetry approach to composite orders has been derived[18], and composite orders have been discussed as a potential class of hidden orders[8, 19].

For ferromagnets and ferroelectrics, the order parameters are given by the magnetization \mathbf{M} and polarization \mathbf{P} , being vectorial, i.e., multi-component order parameters. Consequently, composite order describes combinations of $\langle M_\alpha M_\beta \rangle$, $\langle P_\alpha P_\beta \rangle$, $\langle P_\alpha M_\beta \rangle$ ($\alpha, \beta = x, y, z$). We show that, depending on the anisotropy, a composite or multipolar order emerges in the vicinity of a conventional ferromagnetic or ferroelectric phase transition. For cubic crystalline symmetry, we find that cubic ferroelectrics and ferromagnets undergo a Z_2 classification scheme with respect to the type of quadrupole order. Here, the Z_2 classification is a direct consequence of the two possible easy axes for magnetization and polarization in a fourth order theory. Furthermore, we demonstrate that the concept of composite orders can be extended to multiferroic materials, where polarization and magnetization are coupled. In cubic symmetry, this coupling gives rise to three potential composite orders, aligning with the well-known

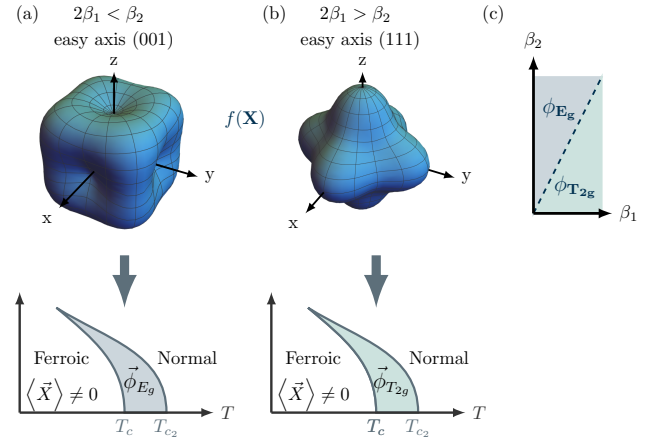


FIG. 1. Z_2 classification of ferromagnets and ferroelectrics. Depending on the easy axis, a quadrupole order transforming as E_g or T_{2g} emerges above the ferroic transition temperature. The anisotropy of the cubic free energy for a vectorial order \mathbf{X} (e.g. magnetization \mathbf{M} or polarization \mathbf{P}) for an easy axis of (a) (100) and (b) (111). (c) illustrates the phase diagram depending on two positive fourth order parameters β_1 and β_2 .

multipole expansion[2, 20, 21]. Hence, we show that the complex phase diagram of magnetic and magnetoelectric materials is strongly dependent on composite orders, challenging the idea of competing orders.

CUBIC FERROMAGNETS AND FERROELECTRICS

The magnetization \mathbf{M} is a pseudo vector, meaning it is even under inversion and odd under time-reversal (Table I). In contrast, the polarization \mathbf{P} behaves as an ordinary vector, being odd under inversion and even under time-reversal. Without lattice anisotropy, a phenomenological theory accounts only for the magnitude of \mathbf{M} and \mathbf{P} , leading to the inversion and time-reversal invariant free energies $f(M) = \alpha(T - T_c)M^2 + \beta M^4$ or

	Time-reversal \mathcal{T}	Inversion \mathcal{P}
Polarization \mathbf{P}	+	-
Magnetization \mathbf{M}	-	+
Quadrupole electric $P_\alpha P_\beta$	+	+
Quadrupole magnetic $M_\alpha M_\beta$	+	+
Composite multiferroic $P_\alpha M_\beta$	-	-
Coupling to strain	+	+
Coupling to toroidal moment	-	-

TABLE I. Transformation behavior under the fundamental symmetries time-reversal and inversion.

$f(P) = \alpha(T - T_c)P^2 + \beta P^4$, with $\alpha, \beta > 0$. At high temperatures $T > T_c$, the free energy is minimized by the trivial solutions $M = 0$ and $P = 0$. Below the critical temperature $T < T_c$, a finite magnetization or polarization appears, indicating a transition into a ferromagnetic or ferroelectric state.

When lattice anisotropy is considered, the free energy also depends on the direction of polarization or magnetization. In cubic symmetry, it is expressed as [22–24]:

$$f(\mathbf{X}) = \alpha(T - T_c)\mathbf{X}^2 + \beta_1 (X_x^4 + X_y^4 + X_z^4) + \beta_2 (X_x^2 X_y^2 + X_y^2 X_z^2 + X_z^2 X_x^2), \quad (1)$$

where $\mathbf{X} = \mathbf{P}, \mathbf{M}$ represents either the magnetization \mathbf{M} or the polarization \mathbf{P} . In the case of antiferromagnets and antiferroelectrics, $\mathbf{X} = \mathbf{M}_1 - \mathbf{M}_2$ or $\mathbf{X} = \mathbf{P}_1 - \mathbf{P}_2$, denoting a difference of contributions from two sublattices. Assuming second-order phase transitions and $\alpha, \beta_1, \beta_2 > 0$, we avoid higher-order terms to achieve minima at finite X_i values. The fourth-order terms β_1 and β_2 determine the anisotropy energy shape. In the ferroic phase ($T < T_c$), the free energy is minimized for a magnetization or polarization along the Cartesian axes (100) if $2\beta_1 < \beta_2$ (Fig. 1(a)). Conversely, for $2\beta_1 > \beta_2$, a magnetization or polarization along the diagonal (111) is energetically favored (Fig. 1(b)). Cubic magnetic anisotropy has long been recognized [25, 26], with Fig. 1(a) describing iron and Fig. 1(b) representing nickel.

We argue that equation (1) also supports a composite order beyond the standard ferroic phases. This is evident when considering bilinears $\phi_k = \sum_{ij} c_{ij}^k X_i X_j$ and expressing the cubic free energy in (1) as a second-order polynomial in ϕ_k . Specifically, for the point group O_h (full cubic symmetry), we define symmetry-adapted bilinears: $\phi_{A_{1g}} = \frac{1}{\sqrt{3}}(X_x^2 + X_y^2 + X_z^2)$, which transforms as the identity representation (A_{1g}), and the quadrupole orders $\phi_{E_g;1} = \frac{1}{\sqrt{2}}(X_x^2 - X_y^2)$ and $\phi_{E_g;2} = \frac{1}{\sqrt{6}}(X_x^2 + X_y^2 - 2X_z^2)$, which transform as the two-dimensional representation E_g . Additionally, $\phi_{T_{2g}} = \sqrt{2}(X_x X_y, X_y X_z, X_z X_x)$ transforms as the three-dimensional irreducible representation T_{2g} .

In terms of these bilinears, equation (1) can be reformulated in two distinct forms. First, using the scalar

$\phi_{A_{1g}}$ and the two-component order parameter ϕ_{E_g} :

$$f(\phi_{A_{1g}}, \phi_{E_g}) = \sqrt{3}\alpha(T - T_c)\phi_{A_{1g}} + (\beta_1 + \beta_2)\phi_{A_{1g}}^2 + \frac{(2\beta_1 - \beta_2)}{2}\phi_{E_g}^2. \quad (2)$$

Second, the free energy (1) can be written in terms of $\phi_{A_{1g}}$ and the three-component order parameter $\phi_{T_{2g}}$:

$$f(\phi_{A_{1g}}, \phi_{T_{2g}}) = \sqrt{3}\alpha(T - T_c)\phi_{A_{1g}} + 3\beta_1\phi_{A_{1g}}^2 + \frac{(\beta_2 - 2\beta_1)}{2}\phi_{T_{2g}}^2. \quad (3)$$

Here, $\phi_{A_{1g}}$, ϕ_{E_g} , and $\phi_{T_{2g}}$ are higher rank order parameters. $\phi_{A_{1g}}$ does not break crystalline symmetries. As $\beta_1 + \beta_2 > 0$, it only lowers the free energy for $T < T_c$ and is therefore not realized. In contrast, for $T > T_c$ the free energy is lowered by a non-zero value of a quadrupole order. For $2\beta_1 < \beta_2$ (easy axis (001), Figure 1(a)), the coefficient of the second order term in the quadrupole order parameter ϕ_{E_g} becomes negative (equation (2)). In contrast, for $\beta_1 + \beta_2 < 0$ (easy axis (111), Figure 1(b)), the coefficient of the second order term in the quadrupole order parameter $\phi_{T_{2g}}$ becomes negative (equation (3)). A corresponding phase diagram is shown in Figure 1(c).

To verify that ϕ_{E_g} gets realized dynamically, we start from the free energy (2), add a gradient term of the form $f_{\text{grad}} = \frac{c\mathbf{X}\nabla^2\mathbf{X}}{2}$ and perform the Hubbard-Stratonovich transformation [27] to obtain

$$f(\mathbf{X}, \phi_{A_{1g}}, \phi_{E_g}) = \mathbf{X} \left(c\nabla^2 + r + \phi_{A_{1g}} + M_1\phi_{E_g;1} + M_2\phi_{E_g;2} \right) \mathbf{X} + \frac{1}{2(\beta_1 + \beta_2)}\phi_{A_{1g}}^2 - \frac{1}{(2\beta_1 - \beta_2)}\phi_{E_g}^2. \quad (4)$$

Details of the calculation are given in the appendix. Here, we absorbed the temperature dependent second order coefficient into $r = \alpha(T - T_c)$. The matrices $M_{A_{1g}}$ and M_i are defined to satisfy $(\mathbf{X} \cdot M_1 \cdot \mathbf{X})^2 = \frac{1}{\sqrt{2}}(X_x^2 - X_y^2) = \phi_{E_g;1}$ and $(\mathbf{X} \cdot M_2 \cdot \mathbf{X})^2 = \frac{1}{\sqrt{6}}(X_x^2 + X_y^2 - 2X_z^2) = \phi_{E_g;2}$, respectively. Furthermore, $\phi_{E_g}^2 = \phi_{E_g;1}^2 + \phi_{E_g;2}^2$. For temperatures above the ferroic transition, $T > T_c$, the fields \mathbf{X} are fluctuating and can be integrated out, leading to the effective free energy in the fields $\phi_{A_{1g}}$ and ϕ_{E_g} ,

$$f = \frac{1}{2\beta} \log \det [c\nabla^2 + r + M_1\phi_{E_g;1} + M_2\phi_{E_g;2} + \phi_{A_{1g}}] + \frac{\phi_{A_{1g}}^2}{2(\beta_1 + \beta_2)} - \frac{\phi_{E_g;1}^2}{2(2\beta_1 - \beta_2)} - \frac{\phi_{E_g;2}^2}{2(2\beta_1 - \beta_2)}. \quad (5)$$

The effective free energy gives rise to a self-consistent equation for the fields $\phi_{E_g;i}$, by evaluating the saddle

point approximation $\frac{\delta f}{\delta \phi_{E_g,i}} = 0$. Assuming slowly varying fields $\phi_{E_g,i} \approx \text{const}$ one obtains a non-trivial solution if (details in the appendix)

$$1 = -\frac{(2\beta_1 - \beta_2)\pi}{2k_B T \sqrt{c^3 \alpha (T - T_c)}}. \quad (6)$$

Equation (6) leads to several key conclusions. First, for the right-hand side to be positive, the condition $2\beta_1 < \beta_2$ must be satisfied, aligning with our initial analysis. Second, the right-hand side yields a real number only for $T > T_c$. Therefore, the transition into the quadrupole phase occurs at a temperature above the critical point for the dipole phase transition, i.e., the onset of (anti)ferromagnetism or (anti)ferroelectricity.

To approximate the transition temperature, we assume the quadrupole transition temperature T_q to be sufficiently close to the dipole transition temperature T_c , i.e., $T_q = T_c + \delta T$ and $T_c \gg \delta T$. Then δT can be approximated from (6) as follows,

$$\delta T = \frac{(2\beta_1 - \beta_2)^2 \pi^2}{4k_B^2 T_c^2 c^3 \alpha}. \quad (7)$$

It follows that the difference between the critical temperatures for the dipole phase T_c and the quadrupole phase T_q depends on the anisotropy squared, $\delta T \sim (2\beta_1 - \beta_2)^2$. Hence, for weakly anisotropic materials $2\beta_1 \approx \beta_2$ the transition temperatures T_q and T_c coincide and the phase transition is not observed. This explains the absence of an observed quadrupolar phase transition in most simple ferromagnets.

While there is no microscopic theory yet for the phenomenological theory developed in this paper, several materials have been verified with a quadrupole transition occurring in the vicinity of a dipole transition. For magnetic materials, magnetic anisotropy is driven by strong spin-orbit interaction. An example for a strong spin-orbit antiferromagnet are rare earth hexaborides, with e.g., DyB₆ having a Néel temperature of $T_c \approx 25$ K and a quadrupole transition at $T_q \approx 30.2$ K [28].

Another promising example is the cubic canted anti-ferromagnet Ba₂MgReO₆. According to magnetization, muon spin relaxation, and neutron-scattering performed by Marjerrison *et al.*, a magnetic phase transition occurs below 18 K, accompanied by a quadrupolar phase between 18 K and ≈ 33 K [29]. Both phase transitions can clearly be seen by peaks in the specific heat. The phase diagram could be verified by synchrotron x-ray-diffraction measurements, reported by Hirai *et al.* [30]. Ba₂MgReO₆ has been investigated more extensively by ab initio methods confirming the strong influence of spin-orbit interaction in the formation of the quadrupole order [31–33]. Similar behavior is also observed in Ba₂ZnReO₆ [29], having a dipole order at $T_c \approx 11$ K and a quadrupole order at ≈ 33 K.

Additionally, the cubic spinel selenide GaNb₄Se₈ shows a quadrupole phase with a transition temperature of $T_q = 50$ K and an antiferromagnetic transition at $T_c = 33$ K [34]. The microscopic theory for this behavior accounts for a combination of strong correlations and spin-orbit interaction.

The composite orders ϕ_{E_g} and $\phi_{T_{2g}}$ break the cubic symmetry and are even under inversion and time-reversal, regardless of its origin (magnetization or polarization), see Table I. Hence, they neither couple linearly to an external electric nor magnetic field. Instead, the electric or magnetic fields couple quadratically to their respective order parameters, which would be visible in a modification of the fourth order susceptibility, as recently discussed on the example of the hidden order phase in URu₂Si₂ [35]. However, ϕ_{E_g} and $\phi_{T_{2g}}$ couple linearly to the respective components of the strain tensor, [36]. Hence, elastic anomalies prior to the phase transition can be expected.

Such behavior has been verified in ferroelectrics. For example, in PbSc_{0.5}Ta_{0.5}O₃ a precursor regime was identified ranging over ≈ 100 K above the ferroelectric transition, exhibiting a softening of the shear elastic constant, which was initially explained by a higher order coupling of coexisting order parameters [37]. In contrast, the composite ferroelectric phase couples linearly to the shear strain, potentially explaining the strength of the effect.

MULTIFERROICS

We continue by extending the model of composite orders to multiferroics [38–44], i.e., materials showing ferroelectric and magnetic ordering simultaneously. As before, we focus on materials where the high temperature phase (before the ferroelectric and magnetic phase transition) is cubic. Such a case is realized in the multiferroic perovskites, e.g. BiFeO₃ [45], which has a cubic crystal structure at temperatures above $\approx 1,103$ K [46]. The free energy of a multiferroic contains a contribution from the ferroelectric phase $f(\mathbf{P})$, the magnetic phase $f(\mathbf{M})$, and their coupling f_c ,

$$f(\mathbf{P}, \mathbf{M}) = f(\mathbf{P}) + f(\mathbf{M}) + f_c. \quad (8)$$

In a time-reversal invariant system with cubic symmetry, the coupling term contains three linearly independent contributions, given by

$$\begin{aligned} f_c = & \gamma_1 (P_x^2 M_x^2 + P_y^2 M_y^2 + P_z^2 M_z^2) \\ & + \gamma_2 (P_x P_y M_x M_y + P_y P_z M_y M_z + P_z P_x M_z M_x) \\ & + \gamma_3 (P_x^2 (M_y^2 + M_z^2) + P_y^2 (M_z^2 + M_x^2) \\ & + P_z^2 (M_x^2 + M_y^2)). \end{aligned} \quad (9)$$

As the formation of composite orders in the magnetic and ferroelectric degrees of freedom has been discussed

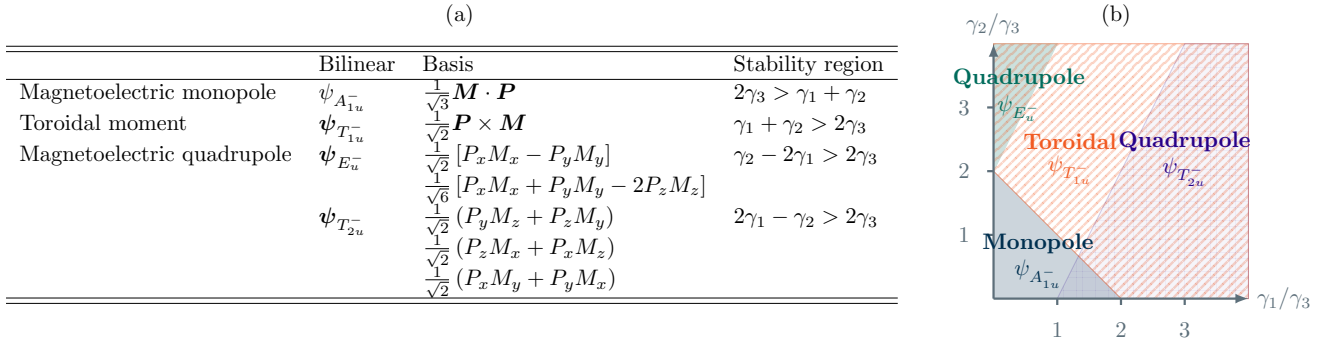


FIG. 2. Composite multiferroic orders in cubic symmetry. (a) Bilinears for composite multiferroic orders and stability region. (b) Phase diagram of composite multiferroic orders.

before, we now focus on the potential of forming multiferroic composites $\langle P_\alpha M_\beta \rangle$, emerging from the multiferroic coupling f_c . As before, we decompose f_c into symmetry adapted bilinears $\psi_k = \sum_{ij} c_{ij}^k P_i M_j$. Due to the individual symmetries of polarization and magnetization, the bilinears ψ_k are odd under time-reversal \mathcal{T} and odd under inversion \mathcal{P} .

In cubic symmetry, the tensor product of the polarization and the magnetization gives $T_{1u}^+ \otimes T_{1g}^- \simeq A_{1u}^- \oplus T_{1u}^- \oplus E_u^- \oplus T_{2u}^-$. These representations can be interpreted in terms of the magnetolectric multipole expansion [2, 20], with A_{1u}^- being the pseudoscalar describing the magnetolectric monopole, T_{1u}^- the toroidal moment vector, and E_u^- and T_{2u}^- the tensor describing the quadrupole magnetic moment. The corresponding symmetry adapted bilinears in \mathbf{P} and \mathbf{M} are given in Table 2(a). As the tensor product of polarization and magnetization can be decomposed into terms transforming as 4 irreducible representations $(A_{1u}^-, T_{1u}^-, E_u^-, T_{2u}^-)$, decomposing the fourth order terms should give rise to four scalars symmetric under all cubic symmetries, $(T_{1u}^+ \otimes T_{1g}^-)^2 \simeq 4A_{1g} \oplus \dots$. However, as the components of \mathbf{P} and \mathbf{M} commute, only 3 linearly independent contributions remain. This becomes apparent from the free energy in equation (9). As a result, the free energy in (9) can be expressed in three, instead of four bilinears (comparable to the Fierz identity in high energy physics). For example, eliminating $\phi_{A_{1u}^-}$ and writing (9) in terms of $\psi_{E_u^-}$, $\psi_{T_{1u}^-}$, and $\psi_{T_{2u}^-}$ the multiferroic coupling f_c is expressed as follows,

$$f_c = \frac{3\gamma_1}{2} \psi_{E_u^-}^2 + \frac{2\gamma_3 - \gamma_1 - \gamma_2}{2} \psi_{T_{1u}^-}^2 + \frac{2\gamma_3 + \gamma_1 + \gamma_2}{2} \psi_{T_{2u}^-}^2. \quad (10)$$

As before, we obtain a free energy with second order contributions in the bilinears, which serve as order parameters of the three corresponding types of composite multiferroic order. These phases can be realized if the coefficient of the second order term becomes negative. Assuming that a fourth order theory is sufficient to describe a system in mind, we require $\gamma_1, \gamma_2, \gamma_3 > 0$. Hence, while

the coefficients before the second order terms in $\psi_{E_u^-}$ and $\psi_{T_{2u}^-}$ are always positive, the toroidal moment $\psi_{T_{1u}^-}$ can emerge as a composite order parameter if $\gamma_1 + \gamma_2 > 2\gamma_3$. Following the theory of composite orders, a macroscopic toroidal moment in the sample [1, 2, 4], can be found as a high temperature phase in a strongly coupled multiferroic material, or at low temperatures in incipient multiferroics. By symmetry, the toroidal order couples to the curl of a magnetic field, $\sim \psi_{T_{1u}^-} \cdot \nabla \times \mathbf{B}$. Furthermore, the toroidal order induces a magnetolectric effect, as can be seen from the polarizability $\mathbf{P} = \chi^e \epsilon_0 \mathbf{E} + \eta \mathbf{B} \times \psi_{T_{1u}^-}$ [1].

In a similar logic as for the toroidal order, different versions of the free energy can be derived to stabilize the monopole or quadrupole orders. For example, by eliminating $\phi_{T_{1u}^-}$ the free energy (9) can be written in terms of $\psi_{A_{1u}^-}$, $\phi_{E_u^-}$, and $\phi_{T_{2u}^-}$,

$$f_c = (\gamma_1 + \gamma_2 - 2\gamma_3) \psi_{A_{1u}^-}^2 + \frac{2\gamma_1 - \gamma_2 + 2\gamma_3}{2} \psi_{E_u^-}^2 + 2\gamma_3 \psi_{T_{2u}^-}^2. \quad (11)$$

As a result, for $\gamma_1, \gamma_2, \gamma_3 > 0$, the free energy (11) gives rise to the magnetolectric monopole phase for $2\gamma_3 > \gamma_1 + \gamma_2$ and the magnetic quadrupole phase for $\gamma_2 > 2(\gamma_1 + \gamma_3)$.

The phase diagram for all four possible composite phases is summarized in Figure 2(b). Interestingly, while there are regions where the monopole or toroidal order can be established independently, the stability regions for the quadrupole orders are found to compete with the toroidal and monopole orders. Under which conditions these orders can be established would require a separate discussion beyond the scope of this paper.

SUMMARY AND OUTLOOK

In summary, we showed the existence of composite orders in (anti)ferromagnetic, (anti)ferroelectric, and multiferroic materials. Starting with cubic ferromagnets and ferroelectrics, we found that a fourth-order Landau expansion of the order parameter gives rise to a

quadrupole order for sufficiently strong cubic anisotropy. For materials with an easy axis along the (100) direction, the quadrupole order exhibits a E_g symmetry while for an easy axis along the (111) axis, a quadrupole order with T_{2g} symmetry is observed. More explicitly, we showed that the quadrupole transition temperature occurs above the dipole transition temperature for an (anti)ferromagnetic or (anti)ferroelectric order, respectively. Using a field theoretical perspective, we find that the difference between dipole and quadrupole transition temperatures depends quadratically on the anisotropy energy. As a result it vanishes for most simple ferromagnets and ferroelectrics. The theory of composite orders derived here is in qualitative agreement with reports about quadrupole orders above magnetic phase transitions, e.g., in $\text{Ba}_2\text{MgReO}_6$ [29, 30], $\text{Ba}_2\text{ZnReO}_6$ [29], GaNb_4Se_8 [34], and RB_6 ($\text{R} = \text{H}, \text{Dy}$) [28]. By symmetry, the E_g and T_{2g} quadrupole orders couple to strain applied to the respective material.

In the second part, we extended the discussion to multiferroics, using the specific example of a coexisting polarization and magnetization in a cubic system. While we primarily focussed on ferromagnetic order, a similar argument holds for antiferromagnetic or more complex magnetic orders. Incorporating a fourth order coupling term in the Landau theory, we showed that the coupling term can be decomposed into four different bilinears describing electromagnetic composite order, being the magnetoelectric monopole (A_{1u}^-), the toroidal order (T_{1u}^-) as well as magnetoelectric quadrupole orders (T_{2u}^- and E_u^-). In terms of the corresponding composite order parameters, the free energy can be formulated in four different variants, giving rise to regions where these orders can emerge at elevated temperatures.

In summary, we could show that the theory of composite orders, can be extended to ferroic materials. Our result shows that the complex phase diagrams in (multi)ferroic and magnetoelectric materials cannot be seen as composed of individual competing orders, but instead as strongly dependent phase transitions. Furthermore, this interpretation becomes interesting when the primary order is not seen at temperature above 0 K, e.g., in incipient ferroelectrics. Still, a composite order above 0 K is allowed. This argument is relevant for the ongoing discussion of hidden order in the condensed matter. For example, in $\text{URu}_{2-x}\text{Fe}_x\text{Si}_2$ a clear phase transition occurs at temperatures above an antiferromagnetic order, in the region around $x \approx 0.1$ [47].

ACKNOWLEDGEMENTS

We acknowledge inspiring discussions with Alexander Balatsky, Nicola Spaldin, Egor Babaev, Erik Fransson, Wolfram Hergert, Paul Erhart, Dominik Juraschek, and Naoto Nagaosa. We are grateful for support by the

Swedish Research Council (VR starting Grant No. 2022-03350), the Royal Physiographic Society in Lund, and Chalmers University of Technology via the department of Physics, and the areas of advance Nano and Materials.

APPENDIX: DECOMPOSING THE MULTIFERROIC COUPLING IN SYMMETRY-ADAPTED BILINEARS

The multiferroic coupling between polarization \mathbf{P} and magnetization \mathbf{M} for cubic symmetry is given in the main text, equation (9). As it contains three linearly independent fourth order terms, four variants can be derived in terms of a decomposition into the four allowed symmetry adapted bilinears $\psi_{A_{1u}^-}$, $\phi_{E_u^-}$, $\phi_{T_{1u}^-}$ and $\phi_{T_{2u}^-}$. We provide these expressions subsequently. Eliminating $\phi_{A_{1u}^-}$, the multiferroic coupling in the free energy is given by

$$f_c^{(1)} = \frac{3\gamma_1}{2}\psi_{E_u^-}^2 + \frac{2\gamma_3 - \gamma_1 - \gamma_2}{2}\psi_{T_{1u}^-}^2 + \frac{2\gamma_3 + \gamma_1 + \gamma_2}{2}\psi_{T_{2u}^-}^2. \quad (12)$$

Eliminating $\phi_{E_u^-}$, one obtains

$$f_c^{(2)} = 3\gamma_1\psi_{A_{1u}^-}^2 + \frac{2\gamma_1 - \gamma_2 + 2\gamma_3}{2}\psi_{T_{1u}^-}^2 + \frac{2\gamma_3 - 2\gamma_1 + \gamma_2}{2}\psi_{T_{2u}^-}^2. \quad (13)$$

Eliminating $\phi_{T_{1u}^-}$, one obtains

$$f_c^{(3)} = (\gamma_1 + \gamma_2 - 2\gamma_3)\psi_{A_{1u}^-}^2 + \frac{2\gamma_1 - \gamma_2 + 2\gamma_3}{2}\psi_{E_u^-}^2 + 2\gamma_3\psi_{T_{2u}^-}^2. \quad (14)$$

Eliminating $\phi_{T_{2u}^-}$, one obtains

$$f_c^{(4)} = (\gamma_1 + \gamma_2 + 2\gamma_3)\psi_{A_{1u}^-}^2 + \frac{2\gamma_1 - \gamma_2 - \gamma_3}{2}\psi_{E_u^-}^2 + 2\gamma_3\psi_{T_{1u}^-}^2. \quad (15)$$

APPENDIX: FIELD THEORY TREATMENT OF COMPOSITE ORDER

We promote the vector \mathbf{X} to a field $\mathbf{X}(\mathbf{r}, t)$. We add a gradient term $\frac{\mathbf{X}\nabla^2\mathbf{X}}{2}$ to the free energy (1) and bring it into the form of equation (2),

$$f(\mathbf{X}) = \frac{c}{2}\mathbf{X}\nabla^2\mathbf{X} + \frac{r}{2}\mathbf{X}^2 + (\beta_1 + \beta_2)(\mathbf{X}^2)^2 + \left(\frac{2\beta_1 - \beta_2}{2}\right)\left([\mathbf{X}\mathbf{M}_1\mathbf{X}]^2 + [\mathbf{X}\mathbf{M}_2\mathbf{X}]^2\right), \quad (16)$$

with c being a constant. For brevity, we introduced $\frac{r}{2} = \alpha(T - T_c)$. The matrices \mathbf{M}_1 and \mathbf{M}_2 are chosen to satisfy, $\mathbf{X}\mathbf{M}_1\mathbf{X} = \frac{1}{\sqrt{2}}(X_x^2 - X_y^2) = \phi_{E_g;1}$ and

$\mathbf{X}M_2\mathbf{X} = \frac{1}{\sqrt{6}}(X_x^2 + X_y^2 - 2X_z^2) = \phi_{E_g;2}$, i.e.,

$$M_1 = \frac{1}{\sqrt{2}} \begin{pmatrix} 1 & 0 & 0 \\ 0 & -1 & 0 \\ 0 & 0 & 0 \end{pmatrix}, \quad M_2 = \frac{1}{\sqrt{6}} \begin{pmatrix} 1 & 0 & 0 \\ 0 & 1 & 0 \\ 0 & 0 & -2 \end{pmatrix}. \quad (17)$$

The corresponding partition function is given by

$$\mathcal{Z} = \mathcal{Z}_0(T) \int \mathcal{D}^3\mathbf{X} e^{-\beta \int d^d x f(\mathbf{X})}, \quad (18)$$

with $\beta = 1/k_B T$. $\mathcal{Z}_0(T)$ accounts for the short-wavelength configurations not contributing to \mathbf{X} [48]. To introduce the quadrupolar order, we apply the Hubbard-Stratonovich transformation. This step is based on the Gaussian integration and the equation,

$$e^{\int d^d x \frac{a}{2} [\mathbf{X}M_i\mathbf{X}]^2} = \mathcal{N} \int \mathcal{D}\phi e^{-\int d^d x \frac{1}{2a} \phi^2 - \mathbf{X}M_i\mathbf{X}\phi}, \quad (19)$$

with \mathcal{N} being a normalization. Identifying $a = -(2\beta_1 - \beta_2)$ for the fields $\phi_{E_g;i}$ and $a = \beta_1 + \beta_2$ for the field $\phi_{A_{1g}}$ leads to the following expression of the partition function,

$$\begin{aligned} \mathcal{Z} = \mathcal{N} \mathcal{Z}_0 \int \mathcal{D}^3\mathbf{X} \mathcal{D}\phi_{A_{1g}} \mathcal{D}\phi_{E_g;1} \mathcal{D}\phi_{E_g;2} \\ \exp \left[-\beta \int d^d x \mathbf{X} \left(\frac{c\nabla^2}{2} + \frac{r}{2} \right) \mathbf{X} + \mathbf{X}^2 \phi_{A_{1g}} \right. \\ \left. + \frac{\phi_{A_{1g}}^2}{2(\beta_1 + \beta_2)} + \mathbf{X}M_1\mathbf{X}\phi_{E_g;1} + \mathbf{X}M_2\mathbf{X}\phi_{E_g;2} \right. \\ \left. - \frac{\phi_{E_g;1}^2}{2(2\beta_1 - \beta_2)} - \frac{\phi_{E_g;2}^2}{2(2\beta_1 - \beta_2)} \right]. \quad (20) \end{aligned}$$

Above the phase transition into the ferroelectric or ferromagnetic state, $T > T_c$, \mathbf{X} is fluctuating and can be integrated out. As a result, one obtains

$$\begin{aligned} \mathcal{Z} = \mathcal{N} \mathcal{Z}_0 \int \mathcal{D}\phi_{A_{1g}} \mathcal{D}\phi_{E_g;1} \mathcal{D}\phi_{E_g;2} \\ \det [c\nabla^2 + r + M_1\phi_{E_g;1} + M_2\phi_{E_g;2} + \phi_{A_{1g}}]^{-\frac{1}{2}} \\ \exp \left[-\beta \int d^d x \frac{\phi_{A_{1g}}^2}{2(\beta_1 + \beta_2)} - \frac{\phi_{E_g;1}^2}{2(2\beta_1 - \beta_2)} - \frac{\phi_{E_g;2}^2}{2(2\beta_1 - \beta_2)} \right]. \quad (21) \end{aligned}$$

This gives rise to the free energy, $f = -k_B T \ln \mathcal{Z}$,

$$\begin{aligned} f = \frac{1}{2\beta} \ln \det [c\nabla^2 + r + M_1\phi_{E_g;1} + M_2\phi_{E_g;2} + \phi_{A_{1g}}] \\ + \frac{\phi_{A_{1g}}^2}{2(\beta_1 + \beta_2)} - \frac{\phi_{E_g;1}^2}{2(2\beta_1 - \beta_2)} - \frac{\phi_{E_g;2}^2}{2(2\beta_1 - \beta_2)}. \quad (22) \end{aligned}$$

This free energy allows us to determine a gap equation for the composite orders $\phi_{E_g;i}$. We use the saddle point

approximation

$$\frac{\delta f[\phi_{E_g;i}]}{\delta \phi_{E_g;i}} = 0. \quad (23)$$

To evaluate the saddle point equation, we use the identity: $\ln \det \hat{G}_i^{-1} = \text{tr} \ln \hat{G}_i^{-1}$ [49] and set $\hat{G}_i^{-1} = c\nabla^2 + r + M_i\phi_{E_g;i}$. We now derive [49],

$$\frac{\delta}{\delta \phi_{E_g;i}} \text{tr} \ln \hat{G}_i^{-1} = \text{tr} \left[\hat{G}_i \frac{\delta}{\delta \phi_{E_g;i}} \hat{G}_i^{-1} \right]. \quad (24)$$

We evaluate the trace, both in matrix space and in operator space ($\text{tr} \hat{A} = \sum_{\mathbf{k}} \langle \mathbf{k} | \hat{A} | \mathbf{k} \rangle$). We obtain for the two components of the quadrupole order,

$$\text{tr} \left[\hat{G}_1 \frac{\delta \hat{G}_1^{-1}}{\delta \phi_{E_g;1}} \right] = \int \frac{d^d k}{(2\pi)^3} \frac{2\phi_{E_g;1}}{-2(ck^2 + r)^2 + \phi_{E_g;1}}, \quad (25)$$

$$\begin{aligned} \text{tr} \left[\hat{G}_2 \frac{\delta \hat{G}_2^{-1}}{\delta \phi_{E_g;2}} \right] = \int \frac{d^d k}{(2\pi)^3} \\ \frac{18\phi_{E_g;2}}{(-3ck^2 + -3r + \sqrt{6}\phi_{E_g;2})(6ck^2 + 6r + \sqrt{6}\phi_{E_g;2})}. \quad (26) \end{aligned}$$

Close to the phase transition into the quadrupole phase we assume $\phi_{E_g;i} \ll k^4$ for most momenta k in the integral. Hence, we remove $\phi_{E_g;i}$ from the denominator in equations (25) and (26) and obtain the universal equation,

$$\text{tr} \left[\hat{G}_i \frac{\delta \hat{G}_i^{-1}}{\delta \phi_{E_g;i}} \right] = - \int \frac{d^d k}{(2\pi)^3} \frac{\phi_{E_g;i}}{(ck^2 + r)^2}. \quad (27)$$

The corresponding linearized gap equation follows from equations (23), (22), and (27),

$$\phi_{E_g;i} = - \frac{2(2\beta_1 - \beta_2)}{k_B T} \int \frac{d^d k}{(2\pi)^3} \frac{\phi_{E_g;i}}{(ck^2 + r)^2}. \quad (28)$$

To evaluate (28) we assume $\phi_{E_g;i} \approx \text{constant}$. Hence, $\phi_{E_g;i}$ cancels on both sides of (28) and the integration of k on the right hand side can be performed to obtain

$$1 = - \frac{(2\beta_1 - \beta_2)\pi}{2k_B T \sqrt{c^3 r}} = - \frac{(2\beta_1 - \beta_2)\pi}{2k_B T \sqrt{c^3 \alpha(T - T_c)}}. \quad (29)$$

* matthias.geilhufe@chalmers.se

- [1] C. Ederer and N. A. Spaldin, Towards a microscopic theory of toroidal moments in bulk periodic crystals, *Physical Review B* **76**, 214404 (2007).
- [2] N. A. Spaldin, M. Fiebig, and M. Mostovoy, The toroidal moment in condensed-matter physics and its relation to the magnetoelectric effect, *Journal of Physics: Condensed Matter* **20**, 434203 (2008).

- [3] A. S. Zimmermann, D. Meier, and M. Fiebig, Ferroic nature of magnetic toroidal order, *Nature communications* **5**, 4796 (2014).
- [4] N. Talebi, S. Guo, and P. A. van Aken, Theory and applications of toroidal moments in electrodynamics: their emergence, characteristics, and technological relevance, *Nanophotonics* **7**, 93 (2018).
- [5] B. V. Svistunov, E. S. Babaev, and N. V. Prokof'ev, *Superfluid states of matter* (CRC Press, Boca Raton, 2015).
- [6] A. V. Balatsky and J. Boncá, Even- and odd-frequency pairing correlations in the one-dimensional $t - J - h$ model: A comparative study, *Physical Review B* **48**, 7445 (1993).
- [7] E. Abrahams, A. Balatsky, D. J. Scalapino, and J. R. Schrieffer, Properties of odd-gap superconductors, *Physical Review B* **52**, 1271 (1995).
- [8] J. Linder and A. V. Balatsky, Odd-frequency superconductivity, *Reviews of Modern Physics* **91**, 045005 (2019).
- [9] E. Babaev, A. Sudbø, and N. Ashcroft, A superconductor to superfluid phase transition in liquid metallic hydrogen, *Nature* **431**, 666 (2004).
- [10] A. Kuklov, N. Prokof'Ev, B. Svistunov, and M. Troyer, Deconfined criticality, runaway flow in the two-component scalar electrodynamics and weak first-order superfluid-solid transitions, *Annals of Physics* **321**, 1602 (2006).
- [11] E. Babaev, Phase diagram of planar $U(1) \times U(1)$ superconductor: Condensation of vortices with fractional flux and a superfluid state, *Nuclear Physics B* **686**, 397 (2004).
- [12] A. B. Kuklov and B. V. Svistunov, Counterflow superfluidity of two-species ultracold atoms in a commensurate optical lattice, *Physical Review Letters* **90**, 100401 (2003).
- [13] A. Kuklov, N. Prokof'ev, and B. Svistunov, Superfluid-superfluid phase transitions in a two-component Bose-Einstein condensate, *Physical Review Letters* **92**, 030403 (2004).
- [14] E. V. Herland, E. Babaev, and A. Sudbø, Phase transitions in a three dimensional $U(1) \times U(1)$ lattice london superconductor: Metallic superfluid and charge-4e superconducting states, *Physical Review B* **82**, 134511 (2010).
- [15] S.-K. Jian, Y. Huang, and H. Yao, Charge-4e superconductivity from nematic superconductors in two and three dimensions, *Physical Review Letters* **127**, 227001 (2021).
- [16] V. Grinenko, D. Weston, F. Caglieris, C. Wuttke, C. Hess, T. Gottschall, I. Maccari, D. Gorbunov, S. Zherlitsyn, J. Wosnitza, A. Rydh, K. Kihou, C.-H. Lee, R. Sarkar, S. Dengre, J. Garaud, A. Charnukha, R. Hühne, K. Nielsch, B. Büchner, H.-H. Klauss, and E. Babaev, State with spontaneously broken time-reversal symmetry above the superconducting phase transition, *Nature Physics* **17**, 1254 (2021).
- [17] C.-w. Cho, J. Lyu, L. An, T. Han, K. T. Lo, C. Y. Ng, J. Hu, Y. Gao, G. Li, M. Huang, N. Wang, J. Schmalian, and R. Lortz, Nodal and nematic superconducting phases in $NbSe_2$ monolayers from competing superconducting channels, *Physical Review Letters* **129**, 087002 (2022).
- [18] R. M. Fernandes, P. P. Orth, and J. Schmalian, Intertwined vestigial order in quantum materials: Nematicity and beyond, *Annual Review of Condensed Matter Physics* **10**, 133 (2019).
- [19] G. Aeppli, A. V. Balatsky, H. M. Rønnow, and N. A. Spaldin, Hidden, entangled and resonating order, *Nature Reviews Materials* **5**, 477 (2020).
- [20] N. A. Spaldin, M. Fechner, E. Bousquet, A. Balatsky, and L. Nordström, Monopole-based formalism for the diagonal magnetoelectric response, *Physical Review B* **88**, 094429 (2013).
- [21] F. Thöle and N. A. Spaldin, Magnetoelectric multipoles in metals, *Philosophical Transactions of the Royal Society A: Mathematical, Physical and Engineering Sciences* **376**, 20170450 (2018).
- [22] R. M. Geilhufe and W. Hergert, GTPack: A Mathematica Group Theory Package for Application in Solid-State Physics and Photonics, *Frontiers in Physics* **6**, 86 (2018).
- [23] O. V. Barabanov and A. Kosogor, Landau theory of ferroelastic phase transitions: Application to martensitic phase transformations, *Low Temperature Physics* **48**, 206 (2022).
- [24] A. Devonshire, Theory of ferroelectrics, *Advances in physics* **3**, 85 (1954).
- [25] J. D. Kleis, Ferromagnetic anisotropy of nickel-iron crystals at various temperatures, *Physical Review* **50**, 1178 (1936).
- [26] J. H. van Vleck, On the anisotropy of cubic ferromagnetic crystals, *Physical Review* **52**, 1178 (1937).
- [27] A. Altland and B. D. Simons, *Condensed matter field theory* (Cambridge university press, 2010).
- [28] T. Goto, Y. Nemoto, Y. Nakano, S. Nakamura, T. Kajitani, and S. Kunii, Quadrupolar effect of $hob6$ and $dyb6$, *Physica B: Condensed Matter* **281-282**, 586 (2000).
- [29] C. A. Marjerrison, C. M. Thompson, G. Sala, D. D. Maharaj, E. Kermarrec, Y. Cai, A. M. Hallas, M. N. Wilson, T. J. S. Munsie, G. E. Granroth, R. Flacau, J. E. Greedan, B. D. Gaulin, and G. M. Luke, Cubic Re^{6+} ($5d^1$) Double Perovskites, Ba_2MgReO_6 , Ba_2ZnReO_6 , and $Ba_2Y_{\frac{2}{3}}ReO_6$: Magnetism, Heat Capacity, μSR , and Neutron Scattering Studies and Comparison with Theory, *Inorganic Chemistry* **55**, 10701 (2016).
- [30] D. Hirai, H. Sagayama, S. Gao, H. Ohsumi, G. Chen, T.-h. Arima, and Z. Hiroi, Detection of multipolar orders in the spin-orbit-coupled $5d$ mott insulator Ba_2MgReO_6 , *Physical Review Research* **2**, 022063 (2020).
- [31] J. Pásztorová, A. Mansouri Tehrani, I. Živković, N. A. Spaldin, and H. M. Rønnow, Experimental and theoretical thermodynamic studies in Ba_2MgReO_6 —the ground state in the context of Jahn-Teller effect, *Journal of Physics: Condensed Matter* **35**, 245603 (2023).
- [32] M. E. Ketfi, S. S. Essaoud, S. M. Al Azar, A. Y. Al-Reyahi, A. A. Mousa, and N. Al-Aqtash, Mechanical, magneto-electronic and thermoelectric properties of ba_2mgreo_6 and ba_2ymoo_6 based cubic double perovskites: an ab initio study, *Physica Scripta* **99**, 015908 (2024).
- [33] A. Mansouri Tehrani and N. A. Spaldin, Untangling the structural, magnetic dipole, and charge multipolar orders in ba_2mgreo_6 , *Physical Review Materials* **5**, 104410 (2021).
- [34] H. Ishikawa, T. Yajima, A. Matsuo, Y. Ihara, and K. Kindo, Nonmagnetic ground states and a possible quadrupolar phase in $4d$ and $5d$ lacunar spinel selenides GaM_4Se_8 ($M = Nb, Ta$), *Physical Review Letters* **124**, 227202 (2020).
- [35] J. Trinh, E. Brück, T. Siegrist, R. Flint, P. Chandra, P. Coleman, and A. P. Ramirez, Thermodynamic measurement of angular anisotropy at the hidden order tran-

- sition of URu_2Si_2 , *Physical Review Letters* **117**, 157201 (2016).
- [36] M. P. Brassington and G. A. Saunders, Cubic invariants in the Landau theory applied to elastic phase transitions, *Physical Review Letters* **48**, 159 (1982).
- [37] O. Aktas, E. K. H. Salje, S. Crossley, G. I. Lampronti, R. W. Whatmore, N. D. Mathur, and M. A. Carpenter, Ferroelectric precursor behavior in $\text{PbSc}_{0.5}\text{Ta}_{0.5}\text{O}_3$ detected by field-induced resonant piezoelectric spectroscopy, *Physical Review B* **88**, 174112 (2013).
- [38] M. Fiebig, Revival of the magnetoelectric effect, *Journal of physics D: applied physics* **38**, R123 (2005).
- [39] D. Khomskii, Multiferroics: Different ways to combine magnetism and ferroelectricity, *Journal of Magnetism and Magnetic Materials* **306**, 1 (2006).
- [40] R. Ramesh and N. A. Spaldin, Multiferroics: progress and prospects in thin films, *Nature Materials* **6**, 21 (2007).
- [41] M. Fiebig, T. Lottermoser, D. Meier, and M. Trassin, The evolution of multiferroics, *Nature Reviews Materials* **1**, 16046 (2016).
- [42] Y. Tokura, S. Seki, and N. Nagaosa, Multiferroics of spin origin, *Reports on Progress in Physics* **77**, 076501 (2014).
- [43] N. A. Spaldin and R. Ramesh, Advances in magnetoelectric multiferroics, *Nature Materials* **18**, 203 (2019).
- [44] D. Bossini, D. M. Juraschek, R. M. Geilhufe, N. Nagaosa, A. V. Balatsky, M. Milanović, V. V. Srdić, P. Šenjug, E. Topić, D. Barišić, *et al.*, Magnetoelectrics and multiferroics: theory, synthesis, characterisation, preliminary results and perspectives for all-optical manipulations, *Journal of Physics D: Applied Physics* **56**, 273001 (2023).
- [45] J. Wang, J. B. Neaton, H. Zheng, V. Nagarajan, S. B. Ogale, B. Liu, D. Viehland, V. Vaithyanathan, D. G. Schlom, U. V. Waghmare, N. A. Spaldin, K. M. Rabe, M. Wuttig, and R. Ramesh, Epitaxial BiFeO_3 multiferroic thin film heterostructures, *Science* **299**, 1719 (2003).
- [46] M. H. Lee, D. J. Kim, J. S. Park, S. W. Kim, T. K. Song, M.-H. Kim, W.-J. Kim, D. Do, and I.-K. Jeong, High-performance lead-free piezoceramics with high curie temperatures, *Advanced Materials* **27**, 6976 (2015).
- [47] H.-H. Kung, S. Ran, N. Kanchanavatee, V. Krapivin, A. Lee, J. A. Mydosh, K. Haule, M. B. Maple, and G. Blumberg, Analogy between the “hidden order” and the orbital antiferromagnetism in $\text{URu}_{2-x}\text{Fe}_x\text{Si}_2$, *Physical Review Letters* **117**, 227601 (2016).
- [48] F. Schwabl, *Statistical Mechanics* (Springer Berlin Heidelberg, 2006).
- [49] A. Altland and B. D. Simons, *Condensed Matter Field Theory* (Cambridge University Press, 2010).